Mass Spectrometry

DOI: 10.1002/anie.201310493

# On-Line Reaction Monitoring and Mechanistic Studies by Mass Spectrometry: Negishi Cross-Coupling, Hydrogenolysis, and Reductive Amination**

*Xin Yan, Ewa Sokol, Xin Li, Guangtao Li, Shiqing Xu, and R. Graham Cooks**

***Abstract:*** *Reaction monitoring using inductive ESI mass spectrometry allows chemical reactions to be tracked in real time, including air- and moisture-sensitive as well as heterogeneous reactions. Highly concentrated solutions can also be monitored for long periods without emitter clogging. Sheath gas assists in nebulization and a sample splitter reduces the delay time and minimizes contamination of the instrument. Short-lived intermediates (ca. 5 s) were observed in Pd/C-catalyzed hydrogenolysis, and several intermediates were seen in Negishi cross-coupling reactions.*

Reaction monitoring for the purpose of process control is critical to assure quality and purity in the manufacture of chemicals and pharmaceuticals. The detailed information acquired during reaction monitoring can help in elucidating reaction mechanisms.[1] Many monitoring methods—absorption and fluorescence spectroscopy, NMR spectroscopy, and electrochemical methods—are already well-established and widely used.[2] Mass spectrometry (MS) is also useful in reaction monitoring because of its capabilities for structural characterization, and its high specificity, sensitivity, and speed. Recent publications on reaction monitoring using MS show two trends: 1) exploration of various new ionization methods for reaction monitoring[3] (see the Supporting Information for a summary) and 2) insights into organic reaction mechanisms through interception of reactive intermediates.[1] Particular success in the latter endeavor has come from electrospray ionization (ESI) monitoring.[1a,b,e,k,l] However, limitations in existing MS monitoring systems still exist: a) Off-line MS reaction monitoring becomes ineffective when fast reaction kinetics and short-lived reaction intermediates are involved. b) High-salt-containing sample solutions cannot be handled in conventional electrospray ionization (ESI) sources because of the likelihood of clogging of the ESI emitter. c) Heated columns used to vaporize the solution in some systems[3l] might expedite the reaction or lead to side products. d) The open-air environment used in some on-line monitoring systems[3d,e,m] is inapplicable to air-sensitive reactions.

We describe an inductive ESI-MS-based on-line reaction monitoring system (Figure 1) which overcomes these limitations. In this method, a positive potential is pulsed repeatedly to produce transient strong electric fields in the spray solution, thereby resulting in the emission of charged droplets in bursts. The reaction solution is transferred to the emitter-

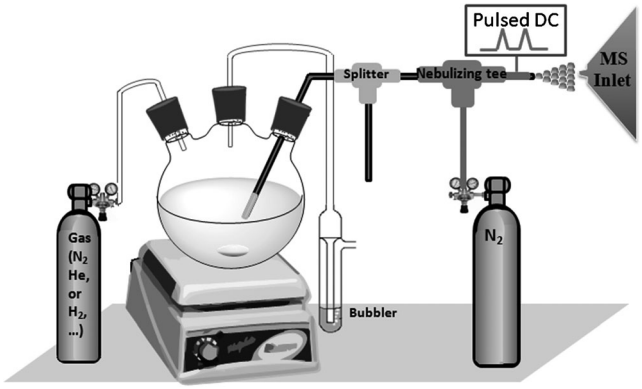


***Figure 1.*** Inductive ESI-MS on-line reaction monitoring system.

spray tip by a capillary under positive gas pressure (e.g. helium as a protective gas if an air-/water-sensitive reaction is involved) and ionized inductively. Note that inductive ESI[4] is a variant of ESI which provides several new capabilities: it is characterized by a remarkable tolerance to matrix and to salt effects and has a high efficiency.[4] Inductive ESI uses a monopolar applied potential, not to be confused with alternating current (AC) electrospray,[5] which uses an alternating and directly applied potential. AC electrospray has definite advantages, but they do not extend to the remote application of the potential or the control of droplet creation, nor do they provide the full immunity to the presence of high salt concentrations or complex matrices seen in inductive ESI. Sheath gas was used to aid in the nebulization process and to minimize variations in droplet size. To allow rapid monitoring, the delay time for sample transfer was reduced to a few seconds by adding a sample splitter, which also minimized contamination of the MS inlet.

Three reactions characteristic of many others important in pharmaceutical synthesis (Scheme 1) were selected for monitoring: a) reductive amination of 4-pyridinecarboxaldehyde with 4-(aminomethyl)pyridine, b) Negishi cross-coupling of 3-bromoquinoline with diethylzinc catalyzed by Pd-PEPPSI (palladium-pyridine enhanced precatalyst preparation, stabi-

[*] X. Yan, E. Sokol, Dr. X. Li, G. Li, Dr. S. Xu, Prof. R. G. Cooks
Department of Chemistry, Purdue University
West Lafayette, IN 47907 (USA)
E-mail: cooks@purdue.edu

[**] We acknowledge funding for this work by the National Science Foundation (CHE 0848650 and CHE 1307264). We also acknowledge funding for a precursor study by Pfizer, Inc. and the efforts of Stephen Brune, Brian Marquez, George Perkins, Scott Bader, Zhongli Zhang, Laura McAllister, Bill Farrell, Matthew Teague, Karen Alsante, Justin Stroh, and Charles Cheng in that prior work.

Supporting information for this article is available on the WWW under http://dx.doi.org/10.1002/anie.201310493.

  

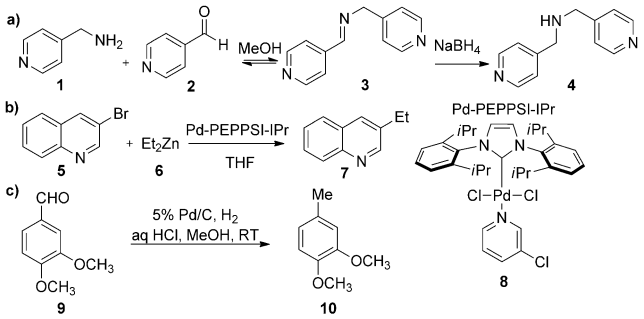


***Scheme 1.*** a) Reductive amination of 4-pyridinecarboxaldehyde; b) Negishi cross-coupling of 3-bromoquinoline with diethylzinc catalyzed by Pd-PEPPSI-IPr; c) Pd/C-catalyzed hydrogenolysis of 3,4-dimethoxybenzaldehyde.

lization, and initiation),[6a] and c) Pd/C-catalyzed hydrogenolysis of 3,4-dimethoxybenzaldehyde.

The reductive amination of 4-pyridinecarboxaldehyde (**2**) with 4-(aminomethyl)pyridine (**1**) was carried out using a one-pot two-step procedure to produce bis((pyridin-4-yl)methyl)amine (**4**). Selected ion chronograms (see Figure S1 in the Supporting Information) record the dynamic changes in ion abundances of reagent **1**, intermediate **3**, and product **4.** (For the corresponding time-resolved mass spectra, see Figure S2 in the Supporting Information.) The kinetic progression of reductive amination can be clearly seen in this data. The first condensation step occurs very fast: once **2** had been added to the solution of **1**, it took less than 1 min for the reaction to reach equilibrium. The intermediate **3** was generated simultaneously with the decrease of **1**. The second reduction step was not as fast as the first. The sodiated adducts of **3** appeared quickly upon addition of $NaBH_4$, thus reflecting the change in the solution-phase matrix. The product ion signal rose sharply in the first 0.5 min after addition of the reducing agent, followed by a slower increase. A corresponding decrease occurred in the signal corresponding to intermediate **3**, driving its equilibrium with **1** to the right and depleting **1**. Altogether, it took about 10 min under the chosen conditions for product **4** to reach its highest concentration, as judged by ion intensity. The total monitoring time was 90 min without any clogging in the fused-silica capillary at the high concentrations of reagents representative of industrial interest.

The kinetic data obtained by continuous inductive ESI-MS measurements of the reductive amination reaction were verified by off-line $^1$H NMR spectroscopy (see Figure S3 in the Supporting Information). Inductive ESI-MS provides both continuous and more detailed information on the reaction. This relatively simple reaction allowed validation of the method.

The time lag between the sampling and measurement of compounds in a reaction mixture is an important factor because it affects how quickly an operator can respond to an unexpected situation. However, when it is small, as it is here, its uncertainty is even smaller, and the lag does not affect the accuracy of the kinetic data. To decrease the amount of sample entering the MS while maintaining a short delay time, a three-way sample splitter was added before the nebulizing gas tee. The delay time in the splitter-equipped inductive ESI-MS monitoring system was measured using optimized transfer and splitter capillary dimensions (see Figure S4 in the Supporting Information) as 0.2 min.

After validation of inductive ESI-MS based online monitoring using the model reductive animation reaction, we investigated reactions with more rigorous requirements. The Negishi reaction—the palladium-catalyzed cross-coupling of organohalides with organozinc reagents—is a selective and versatile method for the formation of C–C bonds which has been widely used in the development of medicinal, agricultural, and organic materials.[6b] The reagents involved are highly susceptible to water or oxygen, so the experiment must be performed with their strict exclusion. Moreover, the Negishi reaction is of additional interest because it appears to occur via a series of cascaded reaction intermediates, the instability and transience of which prevents their isolation. In this study, the cross-coupling of 3-bromoquinoline with diethylzinc catalyzed by Pd-PEPPSI-IPr in tetrahydrofuran (THF; Scheme 1) was monitored by inductive ESI-MS (see the Supporting Information for optimization of the ionization when THF was used as the spray solvent).

The kinetics of the cross-coupling of 3-bromoquinoline with diethylzinc is shown in Figure 2, which displays the changing abundances of the ions corresponding to 3-bromoquinoline (*m*/*z* 208), the ligand of Pd-PEPPSI-IPr (*m*/*z* 389), the reaction product 3-ethylquinoline (*m*/*z* 158), and several intermediates (see below). Immediately after the injection of 3-bromoquinoline into the solution of Pd-PEPPSI at 8.4 min, protonated 3-bromoquinoline was detected at *m*/*z* 208 (and 210 not shown). The injection of the diethylzinc reagent at

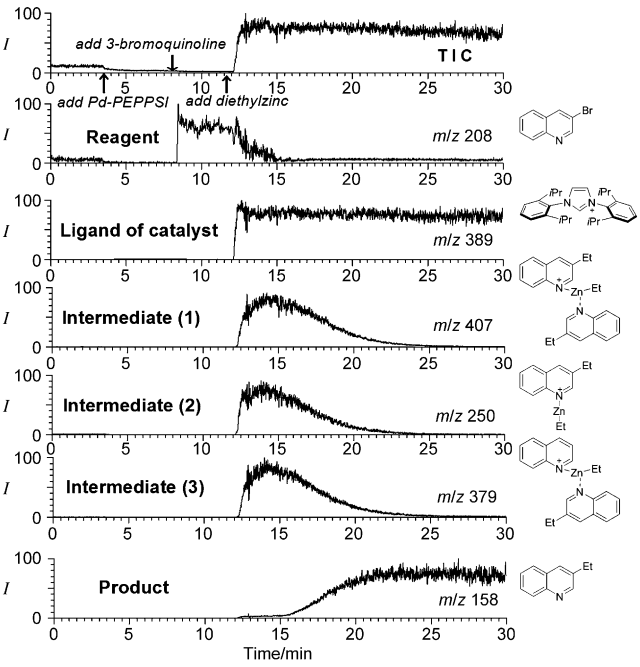


***Figure 2.*** Total ion chronogram and selective ion chronograms of 3-bromoquinoline (*m*/*z* 208), ligand of Pd-PEPPSI (*m*/*z* 389), intermediates (*m*/*z* 407, 250, 379), and the product ethylquinoline (*m*/*z* 158) in the Negishi cross coupling of 3-bromoquinoline with diethylzinc catalyzed by Pd-PEPPSI in THF. *I* = relative abundance.

  

11.6–14 min resulted in the catalyst Pd-PEPPSI being activated from $Pd^{II}$ to $Pd^0$, and ions at *m*/*z* 389 derived from the N-heterocyclic ligand appeared at 12.2 min and quickly increased. Protonated 3-bromoquinoline reagent began to decrease at 12 min, however, the reaction product (seen as protonated 3-ethylquinoline at *m*/*z* 158) did not increase significantly until 3 min later. By scrutinizing time-resolved mass spectra (see Figure S5 in the Supporting Information) and the corresponding ion chronograms, we discerned ions corresponding to three intermediates at *m*/*z* 407, 379, and 250, which appeared and reached their maxima during that 3 min period (Figure 2). The intermediates disappeared, while the product ions at *m*/*z* 158 reached their highest intensity at 25 min. The ions at *m*/*z* 407, 379, and 250 were assigned to quinoline coordinated with ethylzinc (see Figure 2) on the basis of their *m*/*z* values, isotopic distributions, and confirmatory tandem MS (see Figures S6–S8 in the Supporting Information).

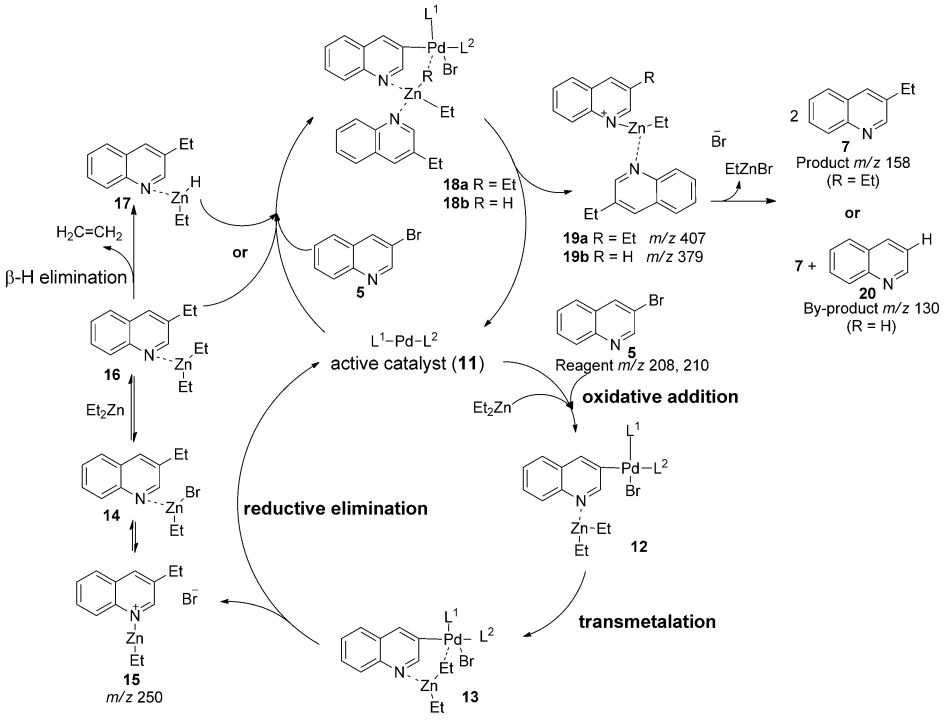


***Scheme 2.*** Proposed mechanism of the Pd-catalyzed Negishi cross-coupling of 3-bromoquinoline with diethylzinc.

Palladium-catalyzed Negishi cross-coupling is regarded as following the pathway: oxidative addition of $R^1X$ to $Pd^0$ to give a $[PdR^1XL_2]$ intermediate, transmetalation from $[M]R^2$ to give $[PdR^1R^2L_2]$, and reductive elimination to afford the product $R^1R^2$ and regeneration of the $Pd^0$ catalyst (see Scheme S1 in the Supporting Information).[6c] Active Pd intermediates without a precharged ligand have not previously been seen by ESI-MS.[7] However, interestingly, the observation of intermediates of quinoline coordinated to ethylzinc complexes suggests that in our experiment the zinc reagent was not released from these complexes throughout the catalytic cycle. A possible pathway consistent with this data is given in Scheme 2 and is described in the Supporting information. A by-product derived from the intermediate at *m*/*z* 379 in this pathway was confirmed in the full-scan mass spectrum and verified by $^1H$ NMR spectroscopy after completion of the reaction and its isolation and purification (see Figures S9 and S10 in the Supporting Information). When the reaction conditions were altered, Pd-containing intermediates were detected in a related reaction (see the Supporting Information).

A question existing in the investigation of intermediates by MS is the extent to which an observed intermediate is the product of the special conditions of the analysis (here small evaporating droplets) versus an accurate representation of an intermediate that occurs in the bulk solution-phase reaction. This question is highlighted by reports on the use of reactions in ESI to generate reaction products on the milligram scale[8] in contrast with the use of desorption electrospray ionization (DESI)-MS as an effective tool for the interception of reaction intermediates[1e–h] (see the Supporting Information for further discussion). One advantage of the inductive ESI-MS-based monitoring system is that it continuously samples aliquots and allows the dynamic changes in the system to be followed. The fact that a series of nested intermediates is observed and that product is only observed as they disappear is strong evidence that solution-phase reactions are being followed. Nevertheless, caution needs to be exercised, because intermediates observed in a reaction might not be species that fall along the pathway that leads directly to product.[9]

Next, we challenged the inductive ESI-MS based reaction monitoring system with a heterogeneous reaction. Pd/C-catalyzed hydrogenation has been widely employed in numerous organic transformations in both academic research and in industry.[10a–c] The reaction commonly proceeds in a $H_2$ atmosphere, which requires the reactor to be held at a positive $H_2$ pressure. Inductive ESI-MS reaction monitoring using a sealed flask at positive pressure allows heterogeneous reactions to be investigated. Here, the Pd/C-catalyzed hydrogenolysis of 3,4-dimethoxybenzaldehyde was monitored by inductive ESI-MS. Selected ion chronograms (Figure 3) and time-resolved mass spectra (see Figure S15 in the Supporting Information) show ions $[\mathbf{9}+H]^+$ at *m*/*z* 167, 0.48 min after injection of reagent **9** into the Pd/C suspension in methanol. Within 0.02 min, a new signal at *m*/*z* 191 appeared, which reached its highest intensity within 0.45 min and disappeared 0.15 min later. Two other new signals at *m*/*z* 235 and 181 were

  

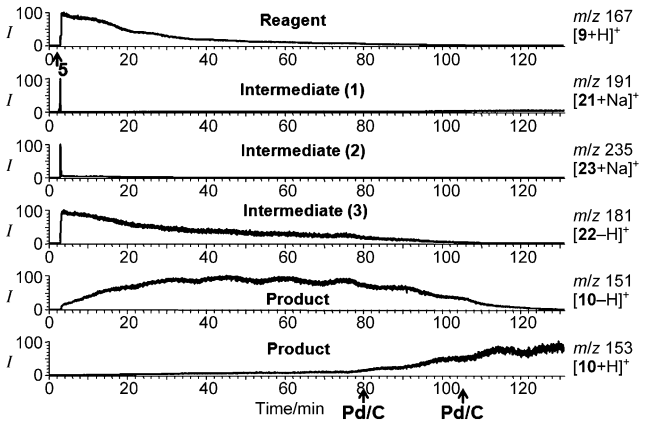


***Figure 3.*** Selective ion chronograms of the reagent **9**, intermediates (1), (2), and (3) assigned (see text) as **11**, **12**, and **13**, and product **10** in the Pd/C-catalyzed hydrogenolysis of 3,4-dimethoxybenzaldehyde over the time range 0–130 min (the arrows indicate when the reagent and excess Pd/C were added).

evident 0.34 min and 0.38 min, respectively, after that at *m*/*z* 191. Just 0.3 min later, the signal at *m*/*z* 235 had disappeared, while the signal at *m*/*z* 181 dominated the reaction mixture spectrum. At the same time, the deprotonated form of the hydrogenolysis product **10** (*m*/*z* 151) began to appear, became the base signal at 18 min, and dominated the spectrum of the reaction product mixture at 75 min. Three separate intermediates (*m*/*z* 191, 235, and 181) were evident during the course of the reaction, as were two forms of the product (*m*/*z* 151 and 153 are the deprotonated and protonated forms of the final product) which are favored at different times (see the Supporting Information for a discussion of the observation of both forms of $[M \pm H]^+$ and the reasons for this in the time-dependent composition of the total reaction mixture).

The detection of transient intermediates in the study of reaction mechanisms is significant, especially because their short lives challenge classical methods of monitoring reactions. Online inductive ESI-MS monitors reactions continuously and provides virtually real-time structural information on the intermediates and products in the mixture, including transient intermediates with half-lives as short as 5 s (see Figure S16, part 1 in the Supporting Information) in reactions that take several hours to complete. The selected ion chronogram in the time interval 2.5–3.5 min (see Figure S16 in the Supporting Information) suggests that the intermediate at *m*/*z* 191 was the first of the three intermediates formed, appearing at almost at the same time as reagent **9** was added. Its signal maximized at 3 min. The intermediate ion at *m*/*z* 235 was followed by one at *m*/*z* 191 in the time range 2.9–3.2 min. The full lifetimes of these two intermediates were both less than 0.3 min. With the decrease of the former intermediates, the intermediate ion at *m*/*z* 181 increased, and the conversion of this intermediate into product **10** then occurred in what appears to be the rate-limiting step.

Pd/C-catalyzed hydrogenolysis of benzaldehydes to methylbenzenes has been described as proceeding via a benzenemethanol intermediate[10d,e] because benzenemethanol has been isolated as an intermediate or as a major by-product. In our experiment, intermediate ions at *m*/*z* 191, 235, and 181 are assigned as sodiated adducts of dimethoxybenzenemethanol (**21**) and of dimethoxybenzaldehyde dimethyl acetal (**23**) and as the hydride abstraction product of dimethoxybenzyl methyl ether (**22**), respectively, as verified by tandem MS and exact mass measurement (see Figure S17 and Table S1 in the Supporting Information). In agreement with the classical benzenemethanol pathway, 3,4-dimethoxybenzaldehyde is first hydrogenated to give dimethoxybenzenemethanol (*m*/*z* 191), then converted into dimethoxybenzyl methyl ether (*m*/*z* 181), and finally the dimethoxytoluene (*m*/*z* 151) product is produced. However, this sequence does not explain the appearance of dimethoxybenzaldehyde dimethyl acetal (*m*/*z* 235). The observed sodiated adduct ions of dimethoxybenzaldehyde dimethyl acetal suggest a second pathway of hydrogenlysis, in which benzaldehyde acetal is an intermediate instead of benzenemethanol. In the recent publication by Hu and co-workers,[10a] a similar benzylaldehyde acetal intermediate was separated and confirmed. The authors noted that when lower alcohols such as methanol (as in our case) and ethanol were used as solvents, only the benzylaldehyde acetal intermediate rather than benzenemethanol was produced as an intermediate. We used the same solvent and conditions as Hu and co-workers, but saw an intermediate, benzenemethanol, which was not seen previously. This is not surprising, as the lifetime of this intermediate was only 5 s, as monitored by the inductive ESI-MS system. Transient intermediates are easily missed in traditional studies of the mechanism. Online inductive ESI-MS monitors reactions continuously and so provides virtually real-time structural information on the intermediates and products in the mixture. As such, it should have great strength in capturing transient intermediates. We suggest a new two-way three-stage pathway involving three intermediates **21**, **22**, and **23** as shown in Scheme 3. In this scheme, the functions of each reaction intermediate are recognized.

In summary, inductive ESI-MS is a versatile method for the direct and continuous monitoring of organic reactions in situ while avoiding the need for physical contact of the high voltage with the reaction solution. Sheath gas was used to assist in the nebulization process and minimize size variation in the droplets. Sample splitting decreased the time offset in the measurement while avoiding contamination of the MS inlet. Three important reactions with different features—reductive amination, Negishi cross-coupling, and Pd/C-cata-

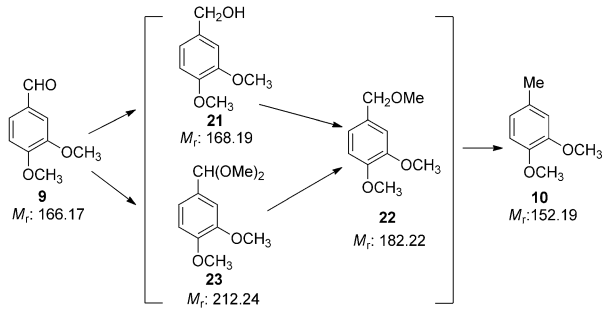


***Scheme 3.*** Two-way three-stage pathway of the Pd/C-catalyzed hydrogenolysis of 3,4-dimethoxybenzaldehyde in methanol.

  

lyzed hydrogenolysis—were successfully monitored by using this system. More interestingly, in the Negishi cross-coupling and Pd/C-catalyzed hydrogenolysis, the observation of new and some very short-lived intermediates and suggestion of their interconnections may give new insights into inconclusive mechanisms or supplement existing mechanisms. The inductive ESI-MS on-line reaction monitoring system provides a general and efficient way to investigate solution-phase organic reaction mechanisms.

## Experimental Section

The configuration of a reaction monitoring system based on inductive ESI is shown in Figure 1. The reaction solution in the sealed vessel was pressurized by helium to ca. 3 psi to allow transfer continuously through the capillary (i.d. 100 μm, length 40 cm) to the emitter-spray tip. A gas bubbler filled with paraffin oil was used to monitor the pressure in the reaction vessel. A tee was added at the front of the capillary tip to introduce sheath gas. A three-way sample splitter was added behind the sheath gas tee. An 8 cm long fused silica capillary (i.d. 100 μm) was connected through the sheath gas tee. The other outlet of the splitter was linked to a fused-silica capillary (i.d. 200 μm, length 8 cm). A home-built power supply provided a positive pulsed output of 2000 Hz and 860 V, which was supplied to an electrode that surrounded the sheath gas line but did not make physical contact. Strong electric fields were produced in the solution inside the emitter and gave rise to bursts of droplets. This procedure resulted in the pulsed emission of charged analytes from the reaction solution at a controlled pulse rate. The spray was directed towards the inlet of the MS, which was ca. 5 mm from the capillary tip. Although not used in this study, the emitted droplets are predominantly positively charged as the pulse is turned on and predominantly negatively charged as it is turned off, thereby allowing rapid successive measurement of positive and negative ion mass spectra.[4] As indicated elsewhere, this has the effect of keeping the emitter from blocking.[4a] A linear ion trap mass spectrometer (LTQ, Thermo Fisher Scientific, San Jose, CA, USA) was used to record positive ion mode mass spectra. The identification of analyte ions was confirmed by tandem mass spectrometry (MS/MS) using collision-induced dissociation (CID).

Received: December 4, 2013
Published online: April 17, 2014

**Keywords:** air-/moisture-sensitive reactions · cross-coupling · mass spectrometry · reaction intermediates · reaction kinetics

[1] a) G. W. Amarante, M. Benassi, H. M. S. Milagre, A. A. C. Braga, F. Maseras, M. N. Eberlin, F. Coelho, *Chem. Eur. J.* **2009**, *15*, 12460 – 12469; b) N. M. M. Nibbering, *Int. J. Mass Spectrom.* **2000**, *200*, 27 – 42; c) M. Vairamani, M. L. Gross, *J. Am. Chem. Soc.* **2003**, *125*, 42 – 43; d) L. S. Santos, L. Knaack, J. O. Metzger, *Int. J. Mass Spectrom.* **2005**, *246*, 84 – 104; e) L. P. E. Yunker, R. L. Stoddard, J. S. McIndoe, *J. Mass Spectrom.* **2014**, *49*, 1 – 8; f) K. Chung, S. M. Banik, A. G. De Crisci, D. M. Pearson, T. R. Blake, J. V. Olsson, A. J. Ingram, R. N. Zare, R. M. Waymouth, *J. Am. Chem. Soc.* **2013**, *135*, 7593 – 7602; g) R. H. Perry, T. J. Cahill, J. L. Roizen, J. Du Bois, R. N. Zare, *Proc. Natl. Acad. Sci. USA* **2012**, *109*, 18295 – 18299; h) R. H. Perry, K. R. Brownell, K. Chingin, T. J. Cahill, R. M. Waymouth, R. N. Zare, *Proc. Natl. Acad. Sci. USA* **2012**, *109*, 2246 – 2250; i) R. H. Perry, M. Splendore, A. Chien, N. K. Davis, R. N. Zare, *Angew. Chem.* **2011**, *123*, 264 – 268; *Angew. Chem. Int. Ed.* **2011**, *50*, 250 – 254; j) P. S. D. Robinson, T.-L. Nguyen, H. Lioe, R. A. J. O'Hair, G. N. Khairallah, *Int. J. Mass Spectrom.* **2012**, *330 – 332*, 109 – 117; k) W. Schrader, P. P. Handayani, J. Zhou, B. List, *Angew. Chem.* **2009**, *121*, 1491 – 1494; *Angew. Chem. Int. Ed.* **2009**, *48*, 1463 – 1466; l) C. A. Müller, A. Pfaltz, *Angew. Chem.* **2008**, *120*, 3411 – 3414; *Angew. Chem. Int. Ed.* **2008**, *47*, 3363 – 3366; for more references, see the Supporting Information.

[2] a) F. Marchetti, G. Pampaloni, C. Pinzino, *J. Organomet. Chem.* **2011**, *696*, 1294 – 1300; b) L. A. Chen, K. Sung, *Org. Lett.* **2009**, *11*, 3370 – 3373; c) C. Felby, B. R. Nielsen, P. O. Skibsted, *Appl. Microbiol. Biotechnol.* **1997**, *48*, 459 – 464; d) O. B. Morozova, S. E. Korchak, R. Z. Sadeev, A. V. Yurkovskaya, *J. Phys. Chem. A* **2005**, *109*, 10459 – 10466.

[3] a) K. Eckart, H. Schwarz, G. Becker, H. Kessler, *J. Org. Chem.* **1986**, *51*, 483 – 486; b) J. Lu, R. Zenobi, *Fresenius J. Anal. Chem.* **2000**, *366*, 3 – 9; c) M. R. Carrasco, M. C. Fitzgerald, Y. Oda, S. B. H. Kent, *Tetrahedron Lett.* **1997**, *38*, 6331 – 6334; d) C. Y. Cheng, C. H. Yuan, S. C. Cheng, M. Z. Huang, H. C. Chang, T. L. Cheng, C. S. Yeh, J. Shiea, *Anal. Chem.* **2008**, *80*, 7699 – 7705; e) Y. Xie, L.-F. He, S.-C. Lin, H.-F. Su, S.-Y. Xie, R.-B. Huang, L.-S. Zheng, *J. Am. Soc. Mass Spectrom.* **2009**, *20*, 2087 – 2092; f) C. Petucci, J. Diffendal, D. Kaufman, B. Mekonnen, G. Terefenko, B. Musselman, *Anal. Chem.* **2007**, *79*, 5064 – 5070; g) E. L. Harry, A. W. T. Bristow, I. D. Wilson, C. S. Creaser, *Analyst* **2011**, *136*, 1728 – 1732; h) Z. Yu, L. C. Chen, R. Erra-Balsells, H. Nonami, K. Hiraoka, *Rapid Commun. Mass Spectrom.* **2010**, *24*, 1507 – 1513; i) T. Y. Chen, C. S. Chao, K. K. T. Mong, Y. C. Chen, *Chem. Commun.* **2010**, *46*, 8347 – 8349; j) A. W. Nørgaard, B. G. Vaz, F. R. Lauritsen, M. N. Eberlin, *Rapid Commun. Mass Spectrom.* **2010**, *24*, 3441 – 3446; k) C. H. Hsieh, C. S. Chao, K. K. T. Mong, Y. C. Chen, *J. Mass Spectrom.* **2012**, *47*, 586 – 590; l) L. Zhu, G. Gamez, H. W. Chen, H. X. Huang, K. Chingin, R. Zenobi, *Rapid Commun. Mass Spectrom.* **2008**, *22*, 2993 – 2998; m) X. Ma, S. Zhang, Z. Lin, Y. Liu, Z. Xing, C. Yang, X. Zhang, *Analyst* **2009**, *134*, 1863 – 1867; n) X. Ma, S. Zhang, X. Zhang, *TrAC Trends Anal. Chem.* **2012**, *35*, 50 – 66.

[4] a) G. Huang, G. Li, R. G. Cooks, *Angew. Chem.* **2011**, *123*, 10081 – 10084; *Angew. Chem. Int. Ed.* **2011**, *50*, 9907 – 9910; b) G. Huang, G. Li, J. Ducan, Z. Ouyang, R. G. Cooks, *Angew. Chem.* **2011**, *123*, 2551 – 2554; *Angew. Chem. Int. Ed.* **2011**, *50*, 2503 – 2506.

[5] N. Chetwani, C. A. Cassou, D. B. Go, H. C. Chang, *Anal. Chem.* **2011**, *83*, 3017 – 3023.

[6] a) I. Larrosa, C. Somoza, A. Banquy, S. M. Goldup, *Org. Lett.* **2011**, *13*, 146 – 149; b) E.-i. Negishi, *Angew. Chem.* **2011**, *123*, 6870 – 6897; *Angew. Chem. Int. Ed.* **2011**, *50*, 6738 – 6764; c) L. Kürti, B. Czakó, *Strategic Applications of Named Reactions in Organic Synthesis*, Elsevier, Amsterdam **2005**, pp. 310.

[7] K. L. Vikse, Z. Ahmadi, C. C. Manning, D. A. Harrington, J. S. McIndoe, *Angew. Chem.* **2011**, *123*, 8454 – 8456; *Angew. Chem. Int. Ed.* **2011**, *50*, 8304 – 8306.

[8] T. Müller, A. Badu-Tawiah, R. G. Cooks, *Angew. Chem.* **2012**, *124*, 12002 – 12005; *Angew. Chem. Int. Ed.* **2012**, *51*, 11832 – 11835.

[9] J. Halpern, *Science* **1982**, *217*, 401 – 407.

[10] a) L. Xing, X. Wang, C. Cheng, R. Zhu, B. Liu, Y. Hu, *Tetrahedron* **2007**, *63*, 9382 – 9386; b) A. Merz, M. Rauschel, *Synthesis* **1993**, 797 – 802; c) K. S. Sagar, C. Chang, W. Wang, J. Lin, S. Lee, *Bioorg. Med. Chem.* **2004**, *12*, 4045 – 4054; d) S. Nishimura, *Handbook of heterogeneous Catalytic Hydrogenation for Organic Synthesis*, Wiley, New York, **2001**, Chap. 5; e) T. J. Connolly, M. Matchett, P. McGarry, R. T. Swann, *J. Med. Chem.* **1996**, *39*, 46 – 55.

  